Journal of Sound and Vibration (2003) **259**(1), 97–118
doi:10.1006/jsvi.2002.5158, available online at http://www.idealibrary.com on IDEAL®

A SELF-EXCITED SYSTEM FOR PERCUSSIVE-ROTARY DRILLING

A. D. Batako, V. I. Babitsky and N. A. Halliwell

*Wolfson School of Mechanical and Manufacturing Engineering, Loughborough University, Leicestershire LE*11 3*TU, UK. E-mail: a.d.l.batako@lboro.ac.uk*

(*Received* 3 *August* 2001, *and in final form* 8 *February* 2002)

A dynamic model for a new principle of percussive-rotary drilling is presented. This is a non-linear mechanical system with two degrees of freedom, in which friction-induced vibration is used for excitation of impacts, which influence the parameters of stick–slip motion. The model incorporates the friction force as a function of sliding velocity, which allows for the self-excitation of the coupled vibration of the rotating bit and striker, which tends to a steady state periodic cycle. The dynamic coupling of vibro-impact action with the stick–slip process provides an entirely new adaptive feature in the drilling process. The dynamic behaviour of the system with and without impact is studied numerically. Special attention is given to analysis of the relationship between the sticking and impacting phase of the process in order to achieve an optimal drilling performance. This paper provides an understanding of the mechanics of percussive -rotary drilling and design of new drilling tools with advanced characteristics. Conventional percussive-rotary drilling requires two independent actuators and special control for the synchronization of impact and rotation. In the approach presented, a combined complex interaction of drill bit and striker is synchronized by a single rotating drive.

1. INTRODUCTION

Drilling of man-made or natural rocks in mining, tunnelling, petroleum exploration, road and construction engineering requires large input of power. The rate of penetration, bit life and cost of maintenance are the major factors of these technologies. These are defined by the resistance of the medium being treated where penetration, separation of chips and friction play the dominant role. Dry friction induces negative side effects, such as wear, squeal, noise and self-sustained vibration leading sometimes to breakage of the system. Friction consumes a great amount of energy imparted to the drilling string, and it often generates a stick–slip motion, which induces torsional vibration.

It is well known that vibration in drilling leads to failure of drill pipes, intensive bit wear and to an increase of overall cost. Drillstring vibration is complex in nature and couples axial, bending and torsional vibration. Investigations of vibration in drilling are carried out generally by studying each aspect independent of others [1–5]. Elsayed *et al.* [6] suggested a model of coupled torsional and axial vibration caused by a fluctuation in the phase angle between surface undulation and cutters. In his work, Brett [7] suggested that bit torque dependence on bit velocity induces identical vibration. Jansen [8–10], has studied different dynamical behaviour of drillstrings such as stick–slip motion, whirling and impact on the borehole. Bit stick–slip motion has been studied by Kyllingstad and Halsey [11]. Jansen and Van Den Steen [8] suggested an active damping system for

0022-460X/02/$35.00

self-excited torsional vibrations and an interesting observation he made is that on impact against a borehole vibration disappears. Measurement of drillstring velocity at the surface and at the bit has shown that drilling systems exhibit properties of torsional oscillation. This means that the surface table rotates at a constant velocity, whilst the bit in the hole has a vibrational motion that consists of constant speed and superimposed torsional vibration [10]. Due to heavy thrust, the bit intermittently cease to turn and throughout the standstill time, the drill pipe is over torqued (up to 10 000 N m [8]) until the bit brakes through freely. At this last instant, the rotational speed of the bit becomes much higher than the velocity at the surface table. This kind of motion has been identified as self-excited vibration [12–14]. The frequency of this type of vibration is about 0·05–0·5 Hz, which is under the first natural frequency of drillstring torsional vibration [10].

To eliminate the above-mentioned negative aspects, improvements are constantly brought in through new concepts of drilling and new designs. These new approaches have to consider the efficient use of energy as an important factor, bringing an increase in bit life, rate of penetration and reduced cost. Rotary, percussive hammer drilling are conventional methods which have had limited success. More recently, the concept of vibro-impact drilling introduced in the last decades has proven to be highly promising.

This paper utilizes the vibration activity of the drill bit for improvement of the drilling process by self-excitation of the imposed vibro-impact action. Conventional rotary-percussive drills require two independent actuators for rotation and impact respectively [15, 16]. Their productive co-operation needs special synchronization of their action, which is difficult to fulfil under real drilling conditions. The paper proposes a *self-exciting oscillatory system* for generating a coupled rotary-impact drilling mode. This provides an adaptive feature to the drilling system, where the intensity of vibro-impact process is regulated by resistance of the medium. The system synchronizes dynamically its stick–slip and impacting action to ensure best use of driving energy. Torsional vibration therefore, is localized at the bit suspension level. Because torsional vibration results from bit stick–slip motion, which is induced by dry friction, the organized correlation of friction properties and driving velocity gives the opportunity to convert a detrimental effect into a useful process.

2. ROTARY AND PERCUSSION DRILLING

Conventional rotary drilling is the most economical in comparison with other methods and typically drills holes of up to 850 mm in diameter. It can drill up to 10 000 m deep in almost all formations. In rotary drilling, cutting of rock is achieved by a rotating drill bit under thrust. Material is removed in the form of dust or chips as a result of the scraping and shearing action of the cutting edges. To obtain big chips and a high rate of penetration, more thrust is required. Hence, this method of drilling suffers from twisting and breakage of the pipes. Drilling systems (see Figure 1) are made of a motor, rotary table, drill pipes (drillstring), drill collar and bit. Through a gearbox, the motor drives the rotary table that rotates the drillstring and the bit. The rotary table is typically a heavy flywheel that is used to smooth irregularities in angular velocity. In some very hard sedimentary formations, the required thrust becomes so great that the bit wear is excessive.

Percussive drilling fragments rock formations by means of blows, which occur only for a fraction of time. This method relies entirely on crack propagation and brittleness of the formation because bit rotation is purely an indexing procedure that occurs when the bit

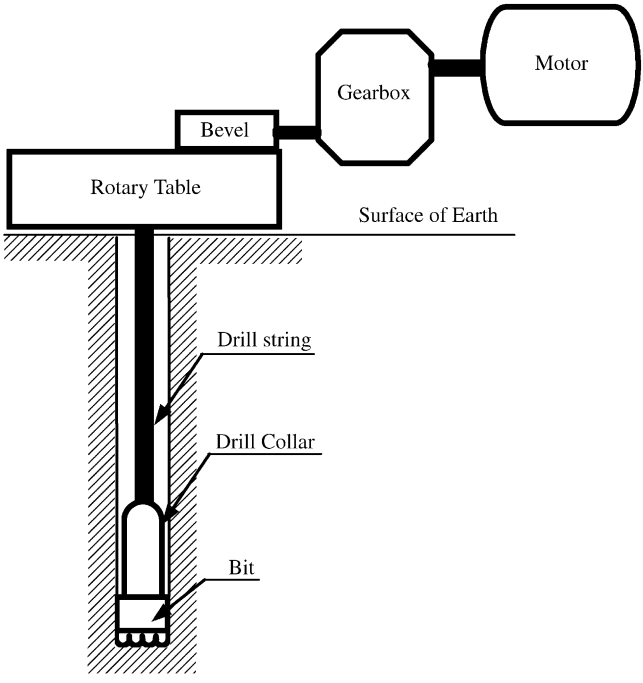

Figure 1. Typical structure of rotary drilling system.

tends to bounce and does not contribute to cutting process. If indexing and thrust are inadequate, the rate of penetration decreases due to small chip formation and energy wasted in bit free rotation [16]. Percussion drilling is preferable in very hard sedimentary rocks because of low bit wear and fast penetration, but this method cannot produce the same rate of penetration as rotary at greater depth. Moreover, percussive drilling can produce only small holes in diameter.

Optimum productivity is possible by combining advantages of both rotary and percussion drilling. Fish [15] described a percussive-rotary drill that was developed first by the Salzgitter Company and then by Hausherr and Nüsse & Gräfer. This type of machine had been mainly used in underground works and had shown to have advantages of both rotary and percussion drills. The Hausherr DK7ES rotary–percussion machine described in reference [15] consists of a vane-type rotary motor, gearbox, rotary shaft, percussion drive with two pistons and a forward shaft with a tapered hole in which the tool is mounted. The machine operates as follows: the rotary motor, located at the rear drives the rotary shaft through the gearbox. The rotary shaft is coupled with the forward shaft of the percussion drive, which has two sliding pistons (hammers). The forward shaft has two shanks upon which each piston strikes. Compressed air is supplied to the percussion drive valve, so that the pistons move in opposite directions, either outwards or inwards. In one direction one piston strikes the first shank, in the other direction, the second piston impacts the second shank. By this blows are delivered to the shaft, which is in constant rotation. The feed screw operated by another air motor secures the advance of the entire drill. The percussion action creates indentation in the formation and eases continuous rotary shear cutting, thus this method requires less thrust and power.

3. MECHANICAL MODEL OF THE SYSTEM

3.1. DESCRIPTION

Figure 2 shows a planar model of the drilling system proposed in this paper. The drive 1 moves with constant linear speed v. A bit 2 with mass m_1 is driven over rough surface through spring 3 with stiffness k_1. Lever 5 carries striker 4 at its upper end and rotates freely about the pin 7 mounted on the drive 1. The other end of the lever is linked from one side to the bit 2 through a secondary spring 6 with stiffness k_2. From the other side, the lever is coupled to the drive by a dashpot with a viscous coefficient c_2. There is dry friction between the bit and the surface. The drive 1 represents the entire drilling system except the drill bit. The velocity v is the linear speed of bit rotation. The intention is to decouple the vibration of the bit from the drill string. This is performed with the help of a special mechanism, which is represented by the springs 3 and 6, the dashpot and the lever 5. There are different ways of implementing this decoupling mechanism. Hydraulic actuators, cams, system of levers, specially designed springs or mechanically reciprocating devices could be used for this purpose.

The entire system operates as follows: when riding over the surface, due to dry friction, the bit moves stepwise sticking and sliding intermittently, thus spring 3 comes into compression and extension alternatively. Such motion evokes deformation of spring 6, and consequently, the striker 4 oscillates around its equilibrium position. Both bodies will vibrate at different frequencies, exhibiting generally complex non-periodical motion. The aim of this structure is to use friction-induced vibration to generate an intensive periodic vibro-impact process with a proper synchronization of the motion of the bit and the striker and to control the stick–slip.

At the beginning, the bit 2 will be at rest until the total pulling force in the springs becomes greater than static friction force acting between the bit and the surface. This period of motionless state is known as the "*stick phase*". Within this phase, the drive moves constantly and spring 3 is extended. Because of the increasing distance between parts 1 and 2, the lever 5 rotates clockwise about the pin because its lower end is attached to the bit through spring 6 with stiffness k_2. Consequently, during the sticking phase the striker moves upwards. The shoulders of lever 5 are of equal length with an angle of 90° between them, and this converts forces applied to the lower end in horizontal direction into vertical forces, which are applied to the striker. As soon as total pulling force exceeds the static friction force, bit 2 moves promptly following the drive. This period of motion is

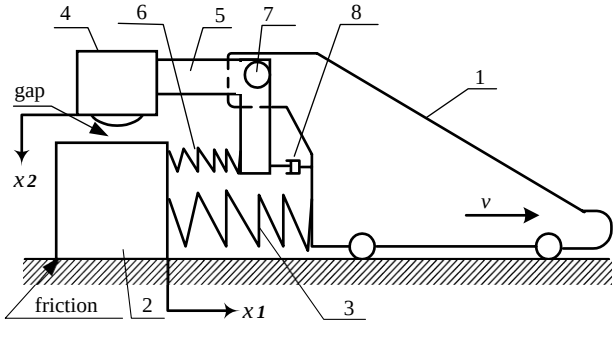

Figure 2. Model of friction-induced self-oscillatory vibro-impact system. 1—Drive with constant velocity v; 2—bit with mass m_1; 3—main spring with stiffness k_1; 4—striker with mass m_2; 5—lever; 6—secondary spring with stiffness k_2; 7—pin; 8—dashpot with viscous coefficient c_2.

called the "*slip phase*". By its sudden motion, the bit pushes the lever anti-clockwise through spring 6. As a result, the striker is forced to hit the bit, which is in motion. During the slip phase, the force in spring 3 is released, but the residual deformation of this element depends on how far the bit has moved towards the drive. The reduction of the forces in the springs by relaxation and additional braking effect due to impact allows the static friction force to become greater than total pulling force. Consequently, the motion slows until the bit stops and the sticking takes place again. The cycle repeats itself and such motion is known as "*stick–slip motion*".

The system is launched with a zero initial condition. Thus, the amplitude of oscillation of the striker increases gradually until it begins to impact the bit when the latter is moving. At impact, the friction force increases sharply and the total pulling force is reduced by relaxation of spring 3. These last two events confine the bit to decelerate and to come to rest. The parameters of the system strongly affect each other therefore, a proper correlation of masses and stiffness in the system is intrinsic for the process to converge to a stable solution. If the required relationship is satisfied, motion of both subsystems synchronize and the entire system comes into a steady state motion and locks into a limit cycle.

3.2. EQUATIONS OF MOTION OF THE SYSTEM

3.2.1. *Characteristics of friction force*

The friction force $F_r(v)$ adopted in this investigation is given by

$$F_r(v) = \mu m_1 g\left(1 - \frac{|v|}{v_{cr}} + \frac{|v^3|}{3v_{cr}^3}\right)\operatorname{sgn}(v), \tag{1}$$

where, v is the sliding velocity, μ is the coefficient of dry friction and g is gravity acceleration. This expression is shown graphically in Figure 3, where v_{cr} is the critical sliding velocity on the falling characteristics beyond which friction force begins to increase (Stribeck velocity [17]), $F_{cr} = F(v_{cr})$ is the corresponding friction force. To obtain self-sustained vibration the sliding velocity must be at some stage on the negative slope or $|v| < v_{cr}$.

3.2.2. *Equations of motion*

The equations of motion of the entire system in Figure 2 are derived relative to drive 1. The bit co-ordinate relative to the drive is x_1 and x_2 the striker co-ordinate. Absolute displacement of the bit is defined by $x = x_1 + vt$. The equations of motion are

$$\begin{aligned} m_1\ddot{x}_1 &= -k_1x_1 - k_2(x_1 - x_2) - F_r(\dot{x}) + \Phi(x_2, \dot{x}_2),\\ m_2\ddot{x}_2 &= -c_2\dot{x}_2 - k_2(x_2 - x_1) - \Im(x_2, \dot{x}_2), \end{aligned} \tag{2}$$

Here, $F_r(\dot{x})$ is the force of friction, $\Phi(x_2, \dot{x}_2)$ is the added friction impulse at the instant of impact of striker on the bit and $\Im(x_2, \dot{x}_2)$ is the impact force of striker 4 colliding with the bit. The friction force is then expressed in the following form:

$$F_r(\dot{x}) = \begin{cases} f_{st}\left(1 - \dfrac{|\dot{x}|}{v_{cr}} + \dfrac{|\dot{x}^3|}{3v_{cr}^3}\right)\operatorname{sgn}(\dot{x}) & \text{for } \dot{x} \neq 0,\\ \min[|k_1x_1 + k_2(x_1 - x_2)|, f_{st}]\operatorname{sgn}(k_1x_1 + k_2(x_1 - x_2)) & \text{for } \dot{x} = 0, \end{cases} \tag{3}$$

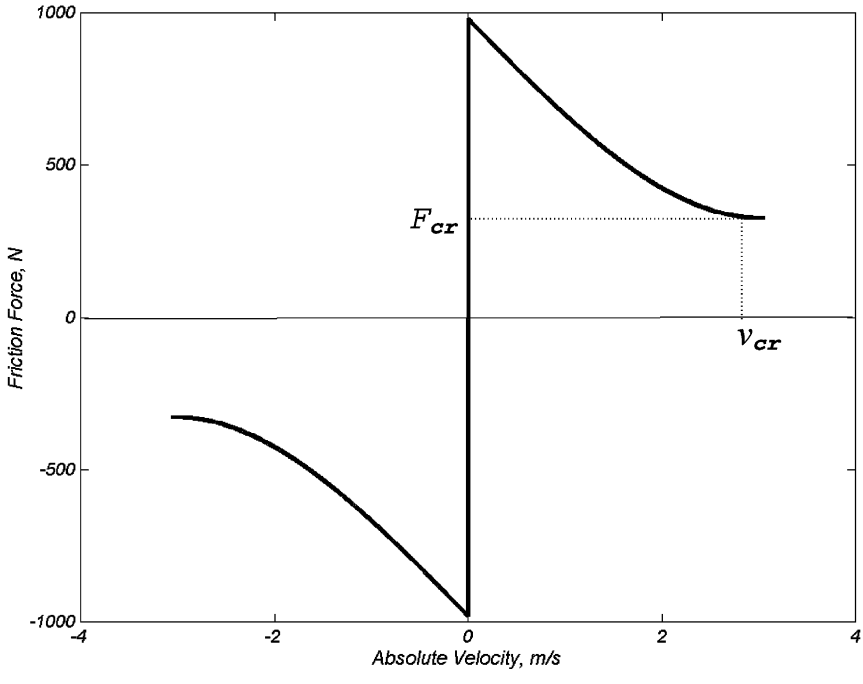

Figure 3. Friction force characteristic.

where $f_{st} = \mu m_1 g$ is the force of static friction. The added friction force due to impact is

$$\Phi(x_2, \dot{x}_2) = \mu \Im(x_2, \dot{x}_2). \tag{4}$$

In this investigation, the coefficient of static friction μ is taken equal to 0·4.

3.2.3. *Analysis of system without impact*

In order to understand the dynamic behaviour of the system, the analysis has been split into two parts: analysis of the system with and without impact. In the absence of impact, the system obtained is a two-degree-of-freedom system, which incorporates dry friction as shown in Figure 4. All referencing numbers in Figure 4 have the same meaning as in Figure 2. In this case $\Im(x_2, \dot{x}_2) = 0$, hence $\Phi(x_2, \dot{x}_2) = 0$ and the equations of motion of the system reads as

$$m_1 \ddot{x}_1 = -k_1 x_1 - k_2(x_1 - x_2) - F_r(\dot{x}), \qquad m_2 \ddot{x}_2 = -c_2 \dot{x}_2 - k_2(x_2 - x_1). \tag{5}$$

The eigenvalue problem for vibration analysis is used to estimate the natural frequencies of the system. Because dry friction has no effect on the system frequency response, the expression of the friction force in equation (5) is neglected to simplify calculation.

3.2.4. *Vibro-impact motion with dry friction*

The structure in Figure 2 is developed to produce a vibro-impact process where striker 4 periodically collides with the bit. Depending on the value of the gap between the bit and striker, the amplitude of oscillation of the striker increases until it starts to hit the bit. The striker–bit contact area is modelled as a visco-elastic material with spring and dashpot in parallel as in references [18–20], where dynamic compliance has been used to define the

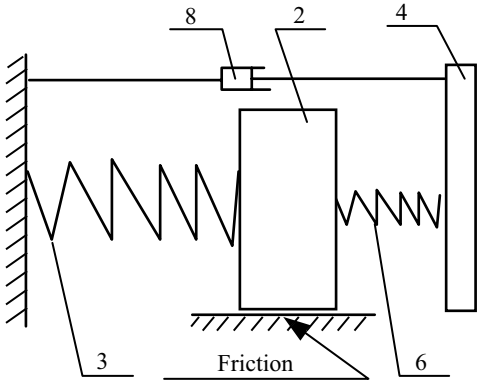

Figure 4. Equivalent model of the system without impact.

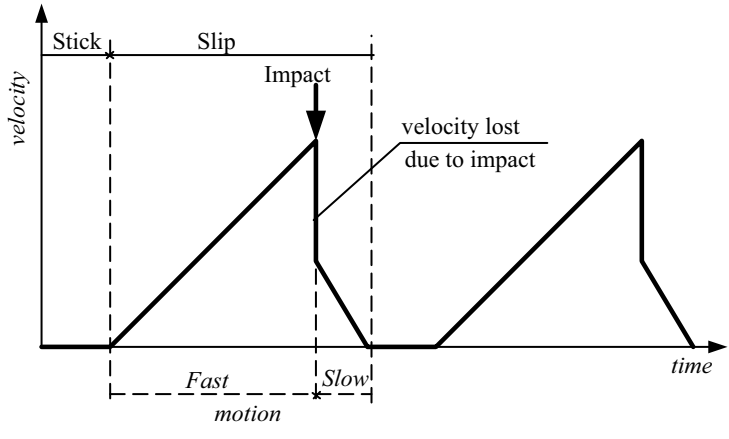

Figure 5. Prescribed working cycle of the system.

impact force as follows:

$$\Im(x_2, \dot{x}_2) = \begin{cases} k_0(x_2 - \Delta) + c_0\dot{x}_2 & \text{for } x_2 \geqslant \Delta \quad \text{and} \quad \Im(x_2, \dot{x}_2) > 0, \\ 0 & \text{for } x_2 \geqslant \Delta \quad \text{and} \quad (x_2, \dot{x}_2) < 0, \\ 0 & \text{for } x_2 < \Delta, \end{cases} \tag{6}$$

where k_0 is contact stiffness of the bit and c_0 is contact damping and Δ is the initial gap between bit and striker.

The impact on the bit steeply increases the friction force and the total pulling force is reduced by relaxation of spring 3. Consequently, the force of friction becomes greater than the force of spring deformation.

Figure 5 shows the working cycle of the entire system. When the spring force exceeds static friction, the bit is propelled and accelerates, then striker 4 imparts a blow on it. Consequently, the velocity diminishes quickly, and the bit comes to a standstill. To implement such a motion as described above, an impact must occur at a given time in the period of motion. Empirically, it was found that to secure the above-described sequences, the frequency ratio ω_2/ω_1 must be between 0·75 and 0·8 where ω_1 and ω_2 are, respectively,

natural frequencies of the subsystem bit-spring 3 and the subsystem striker-spring 6. Accordingly,

$$\omega_1 = \sqrt{k_1/m_1}, \quad \omega_2 = \sqrt{k_2/m_2} \quad \text{and} \quad \omega_2/\omega_1 \in [0{\cdot}75-0{\cdot}8].$$

4. NUMERICAL SIMULATION

A MatLab-Simulink software package was used for numerical simulation of the equations of motion of the system. This package offers a range of facilities for dynamic simulation of mathematical models. In Simulink, differential equations are represented in a set of diagrams similar to solving differential equations on an analogue computer. Solutions of the system are visually displayed dynamically in the form of a plot on an oscilloscope and data may be stored in matrix form for further manipulation in MatLab or other software.

4.1. THE SIMULINK MODEL

To solve the equations of motion of the system, a Simulink model was developed and partitioned into four sections. The first section computes solutions of the subsystem bit-spring 3, the second section computes the solution of the subsystem striker-spring 6 (see Figure 2). These two sections are coupled through spring 6, which drives the striker. The third and the fourth sections are more complex because of decision making on the state of the friction force. A series of logical and relational operators are set to determine the actual state of bit 2. At each integration step, the current value of bit velocity is compared with zero. If it is not equal to zero then the friction force is calculated as a function of absolute velocity given by first part of equation (3). As soon as the velocity becomes zero, the current value of spring force is estimated. This value is then compared to the static friction force to decide which of these two (in absolute values) should be taken as actual friction force. The friction force is set to be the smaller of these two values. Subsequently, the sign of spring deformation is determined and the direction of friction force is set opposite to spring deflection. The output of the last two sections is either dynamic friction force if the velocity differs from zero or the minimum force between static force and force of deflection in springs if the velocity is zero. Upon making this decision, integration continues.

For greater accuracy, a Runge–Kutta fourth and fifth order is used in this simulation. In Simulink, this method has variable step of integration that allows special events to be tracked. It automatically reduces the step size where needed and this feature has been used to accurately capture the zero crossing of the bit velocity, and the interaction of striker with the bit.

4.2. RESULTS

In order to follow the evolution of the process, the simulation is split into two levels. First, the simulation has been carried out to study frequency response of the system without impact. Second, an impact is added and the entire system is simulated. All aforementioned steps are carried out with variation of mass ratio, stiffness and damping.

4.2.1. *Simulation of the system without impact*

Normal frequencies of the system without impact ($\Im(x_2, \dot{x}_2) = 0$ and $\Phi(x_2, \dot{x}_2) = 0$) were obtained using an eigenvalue problem approach. This allows checking the correctness of

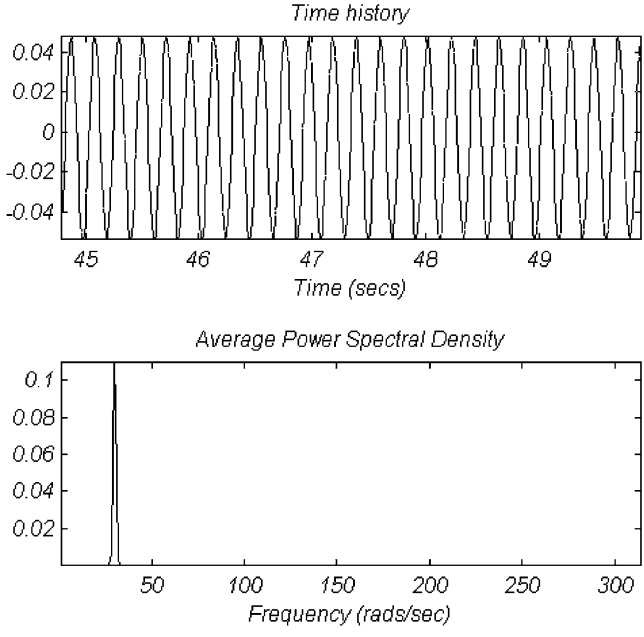

Figure 6. Displacement and frequency spectrum of bit.

the Simulink model and the system frequency response. To study the response of the system, the mass ratio $\beta = m_2/m_1$ is set constant ($\beta = 0{\cdot}4$) and other parameters are varied. Results in Figure 6 were obtained for the following parameters: driving velocity $v = 1{\cdot}5\,\text{m/s}$, $m_1 = 250\,\text{kg}$, $m_2 = 100\,\text{kg}$, $k_1 = 15\,6250\,\text{N/m}$, $k_2 = 35\,156\,\text{N/m}$ and $c_2 = 250\,\text{N s/m}$. The natural frequencies of the bit on spring 3 for this case is $\omega_1 = 25\,\text{rad/s}$ and for the striker on spring 6 is $\omega_2 = 18{\cdot}75\,\text{rad/s}$. From equation (5) using the eigenvalue method the following system normal frequencies were obtained: $\omega_{n1} = 29{\cdot}34\,\text{rad/s}$ and $\omega_{n2} = 15{\cdot}97\,\text{rad/s}$. Simulation has shown that the entire system synchronizes at $29{\cdot}29\,\text{rad/s}$, which is the second normal frequency. This is seen from Figure 6, which displays the bit relative displacement and its frequency spectrum and Figure 7 depicts the period of motion. The striker motion exhibits the same periodic properties.

Figure 8 shows the bit relative velocity with the development of self-excitation and its stabilization. It is seen that relative velocity goes from zero (zero initial condition) and increases until it reaches the value of driving velocity. Once both velocities are equal, further increase of relative velocity is impossible because the friction force reaches its static value and holds the bit, which enters the sticking phase. In Figure 9, the evolution of the process displays one attractor, which appears at the outer loop where the system locks into a limit cycle.

The evolution of friction force is depicted in Figure 10. It was assumed that the bit is at rest from the beginning but in an actual drilling process, the bit, rotating at velocity v is brought to contact with the medium. Therefore, at the instant of contact (time $t = 0$), the friction force is evaluated by equation (3) and is less than static friction. It is seen from this picture that the friction force increases until the value of static friction force is reached and the sign of the force changes to opposite. Because in terms of absolute displacement the bit does not move backwards, the system operates only on the positive side of the friction characteristic.

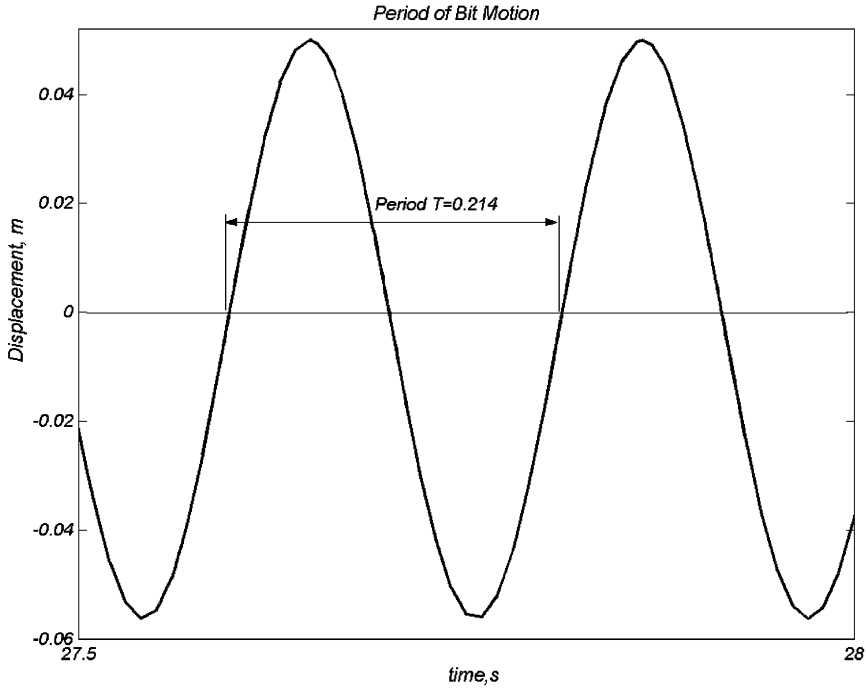

Figure 7. Relative periodic motion of bit.

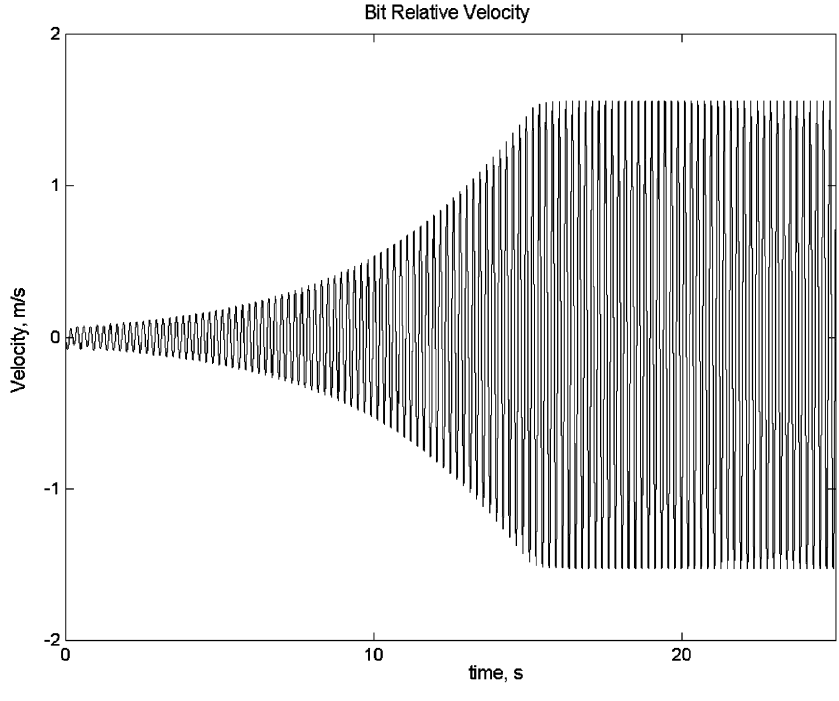

Figure 8. Bit relative velocity showing the self-excitation and stabilization of self-oscillatory process.

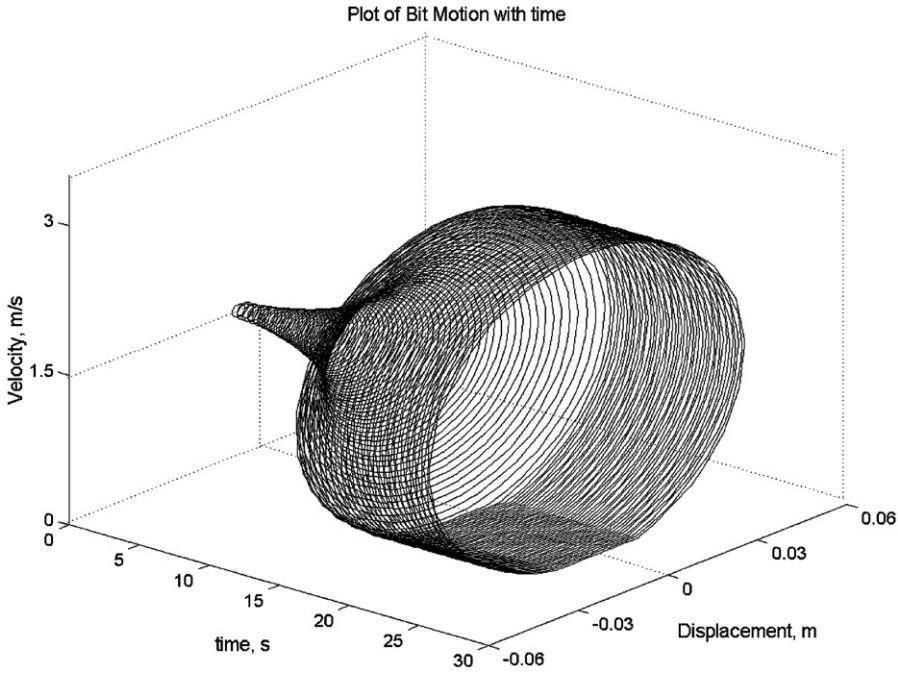

Figure 9. Phase portrait of bit stick–slip motion tending to the limit cycle.

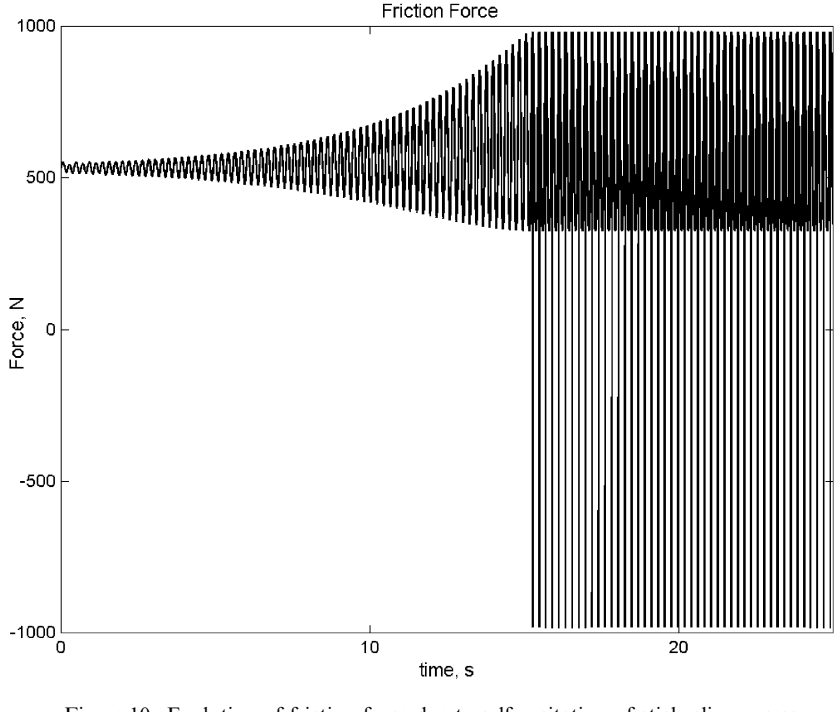

Figure 10. Evolution of friction force due to self-excitation of stick–slip process.

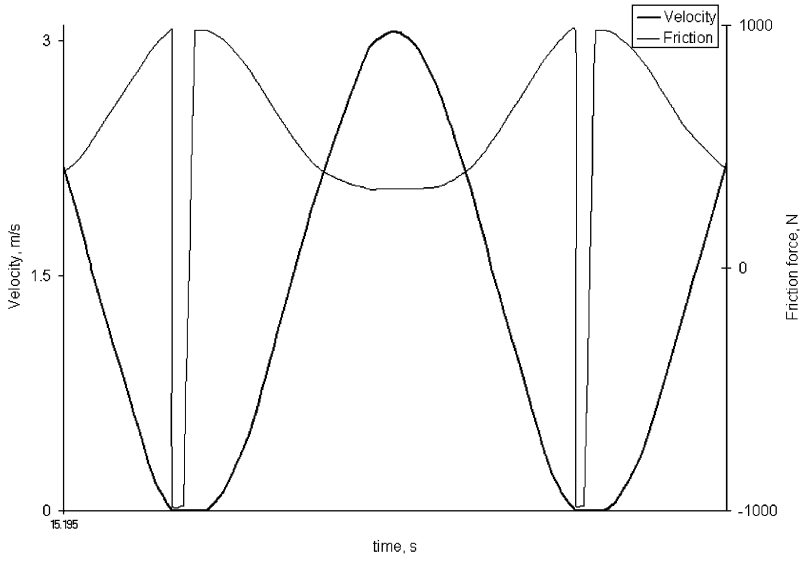

Figure 11. Friction force and bit velocity in steady state periodic process.

In Figure 11, the friction force is plotted together with velocity when the system is in steady state motion. Once the static force is reached, the sign of the friction force changes. At this instant, the sticking phase occurs (bit at rest) and the friction force is evaluated as the minimum force between that of static friction and the force of the spring deformation. The total pulling force of spring deformation will then grow until it exceeds static friction force and the bit begins to accelerate.

4.2.2. *Simulation of vibro-impact motion*

In vibro-impact motion as described in section 3.1, the striker 4 periodically imparts blows on the bit. Equations (2), (3) and (6) govern the motion of the entire system. In equation (6), values of the contact stiffness k_0 and contact damping c_0 are set to 9×10^6 N/m and 0·1 N s/m respectively [20]. Depending on the amount of damping, stiffness and mass ratio, the system exhibits different behaviour including bifurcation.

Empirically, it has been defined that in order to synchronize the bit stick–slip motion with periodic impacts of the striker, the frequency ratio ω_2/ω_1 must be in a range of 0·75–0·8. An adequate correlation of damping in the system and mass ratio is intrinsic for obtaining a steady stable periodic motion with impact occurring at maximum or just after maximum bit velocity. The simulation has been carried out with the same parameters as in the case without impact.

In vibro-impact motion, the system resonant frequency is less than the one obtained without impact. This is because impact does not only reduce the velocity but it retards the motion with increased friction force, which holds the bit throughout the time of impact. In impact regime, the system frequency response is 27·45 rad/s.

Figure 12 displays the build up of the process and it can be seen that the settling time is shorter in comparison with the motion without impact (see Figure 8). This is because impact induces an additional friction force which only acts during the impact time. Consequently, a premature sticking occurs and steady state motion is reached earlier (few cycles). Figure 13 presents the period of motion in impact regime where steep reduction of

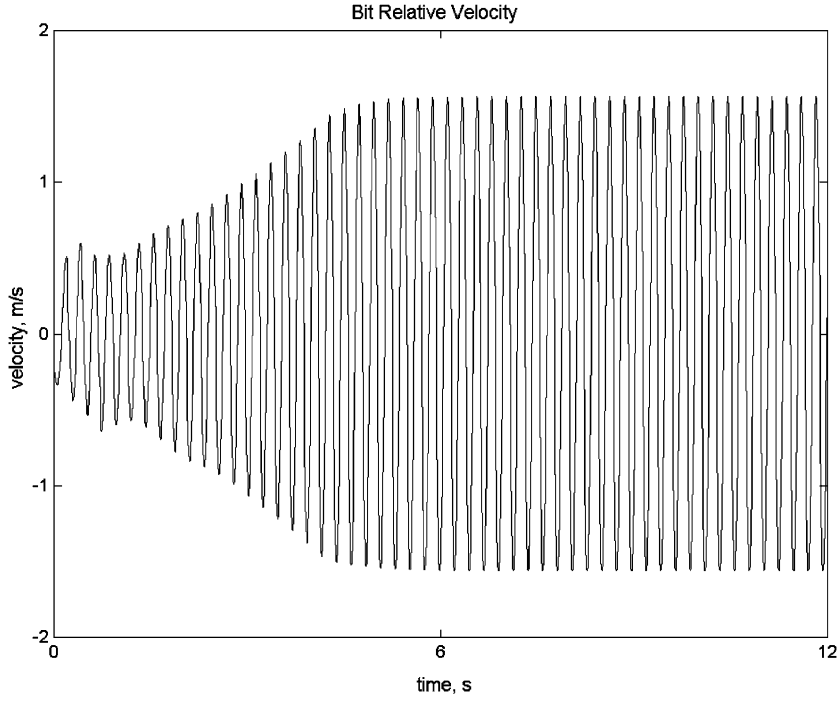

Figure 12. Velocity of bit periodic motion with imposed impacts.

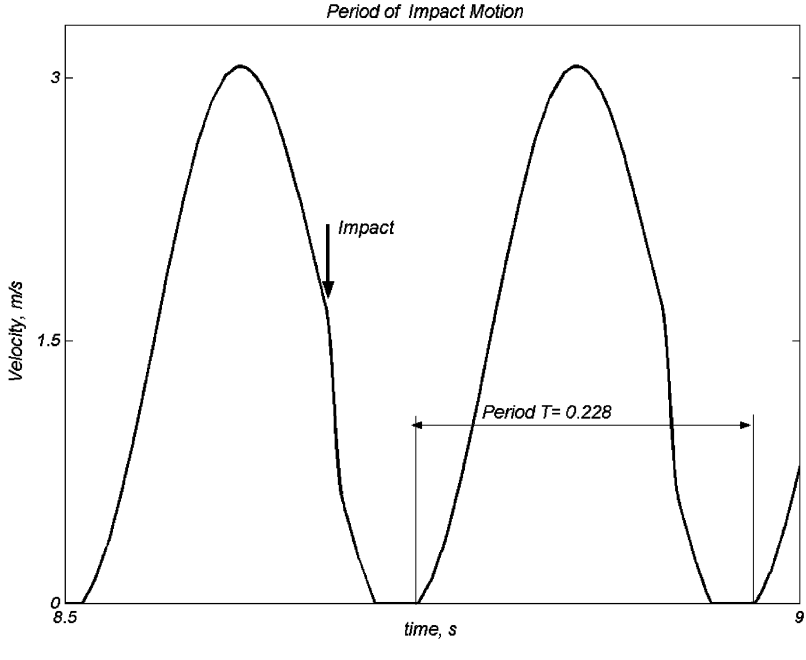

Figure 13. Bit relative velocity in impact regime.

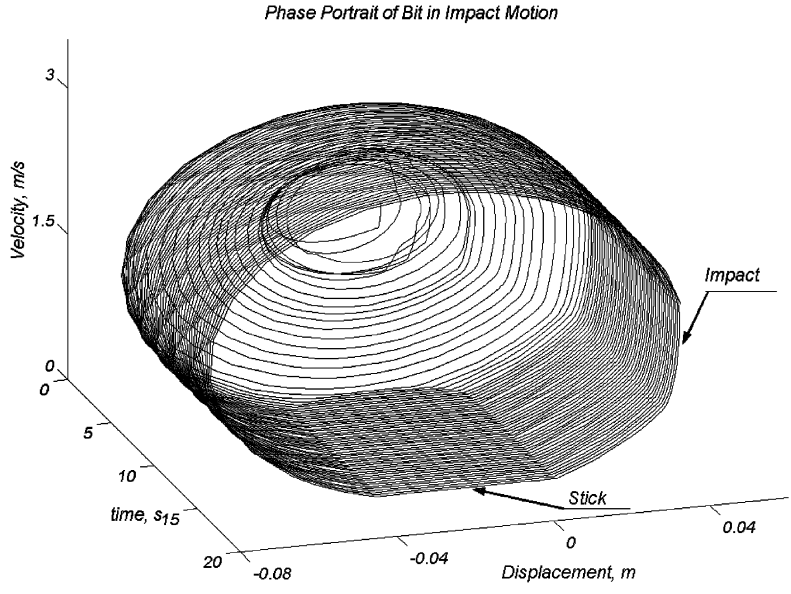

Figure 14. Plot of bit motion with time.

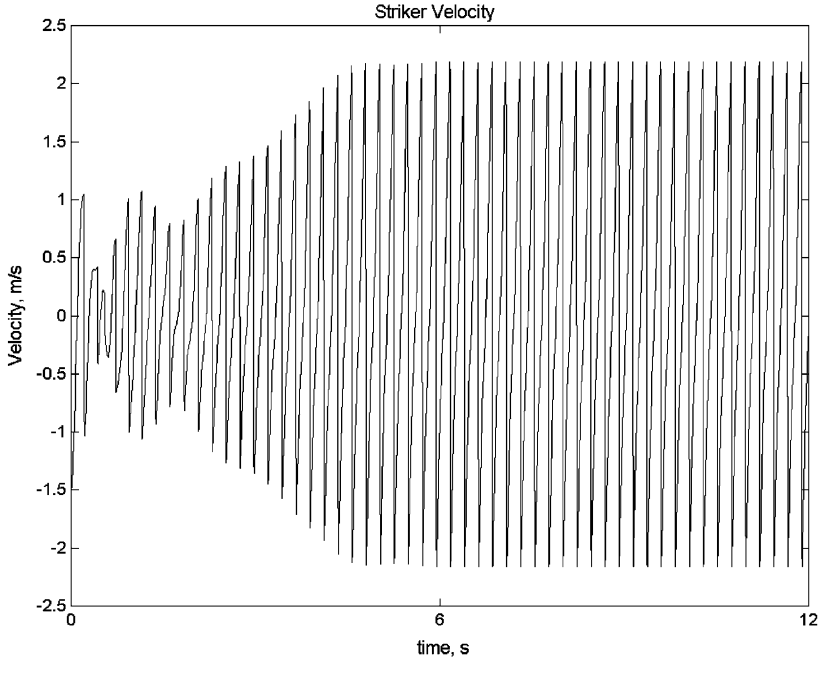

Figure 15. Development of striker velocity in time.

velocity is seen. Figure 14 is a 3-D-phase plot of the bit motion with impact. Here, we see that the system is quickly attracted to the limit cycle.

The striker exhibits the same periodic behaviour as the bit because bit response impels a similar reaction in the striker subsystem. Figure 15 shows that the change in striker

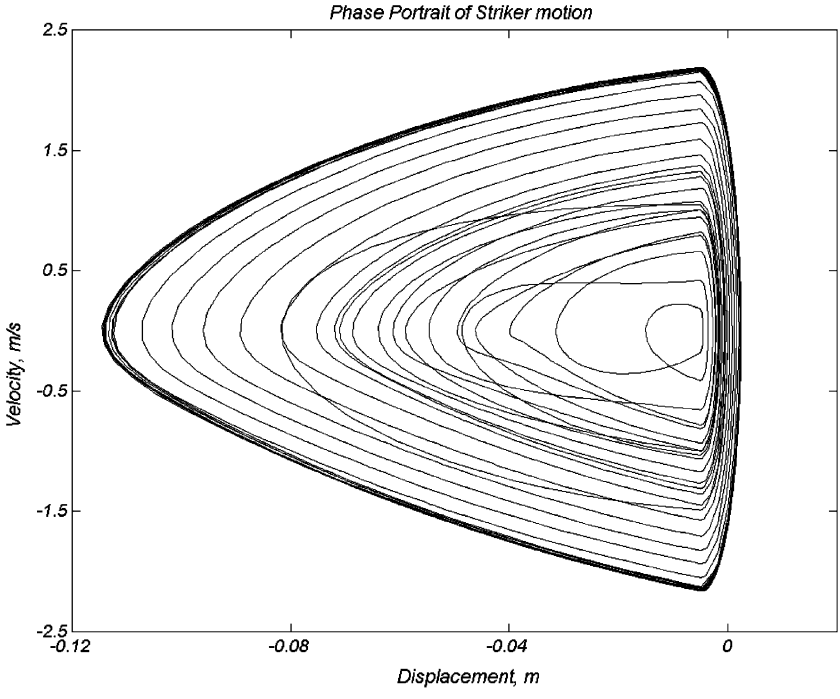

Figure 16. Phase portrait of striker motion.

velocity is about 4 m/s. The phase plot of the striker motion is shown in Figure 16, with reference to this figure the striker is attracted towards a limit cycle where the steady state motion is reached.

Figure 17 presents the synchronized motion of both the bit and striker and their respective velocities and Figure 18 shows the absolute displacement of the bit during stick–slip motion.

4.2.3. *Influence of mass ratio*

The mass ratio β is of importance in obtaining a stable vibro-impact process. For different values of β, the system displays a range of behaviour, including bifurcation.

For $\beta \in [0{\cdot}1, 0{\cdot}2]$: Figures 19 and 20 show the phase diagrams of the bit and striker motion for $\beta = 0{\cdot}1$ respectively. With reference to Figure 19 one sees that the impact is very weak because the striker is light and it performs an unnecessary additional oscillation during the first half cycle following the impact. This is observed in the lower branch of the phase diagram of the striker motion in Figure 20.

For $\beta \in [0{\cdot}25, 0{\cdot}5]$: the system produces a stable vibro-impact process. Figures 21 and 22 are obtained with $\beta = 0{\cdot}3$ and display the phase diagram of the bit and striker respectively. As shown in above-mentioned pictures, this interval of values of β secures consistent solutions of the system and gives stable vibro-impact process.

For $\beta \in [0{\cdot}6, 1]$: the motion is periodic but the solutions of the system are unstable. This behaviour is depicted in Figures 23 and 24. With reference to these figures there is no sticking because the system develops a small velocity, which does not reach zero sliding velocity. Therefore, the velocity increases very slowly until the system reaches a steady state motion only in the slip phase. Figure 25 shows the velocity of the bit for this case.

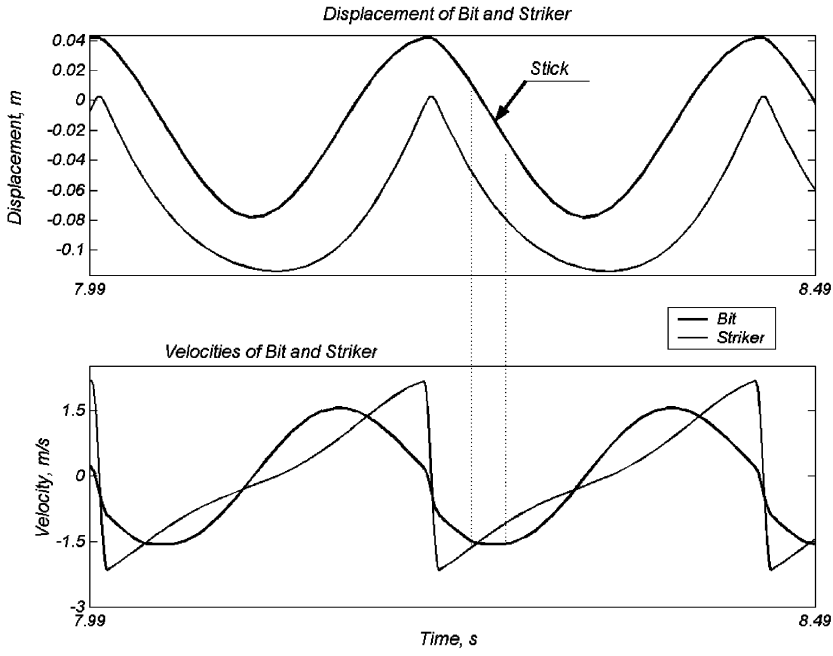

Figure 17. Displacement and velocities of bit and striker in steady state periodic process.

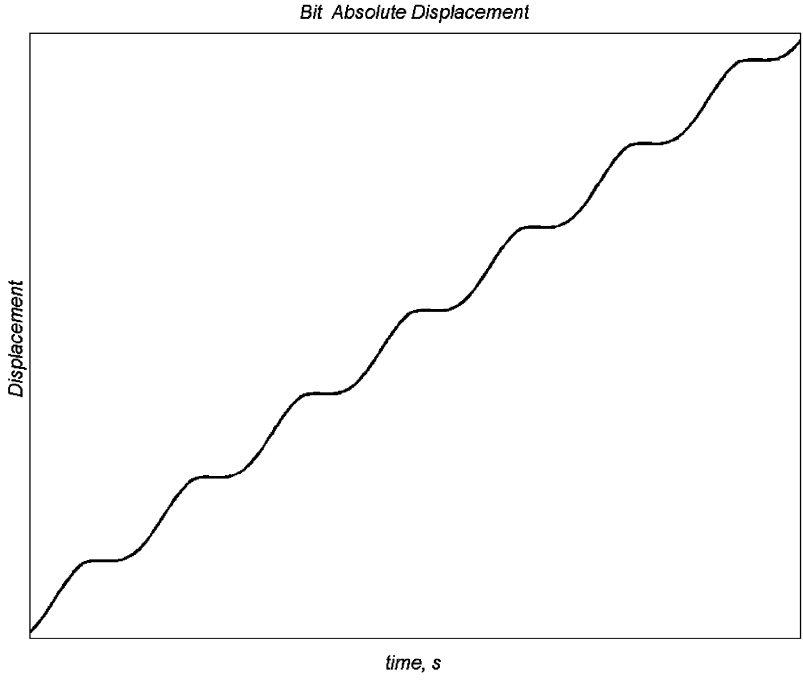

Figure 18. Absolute displacement of bit in time.

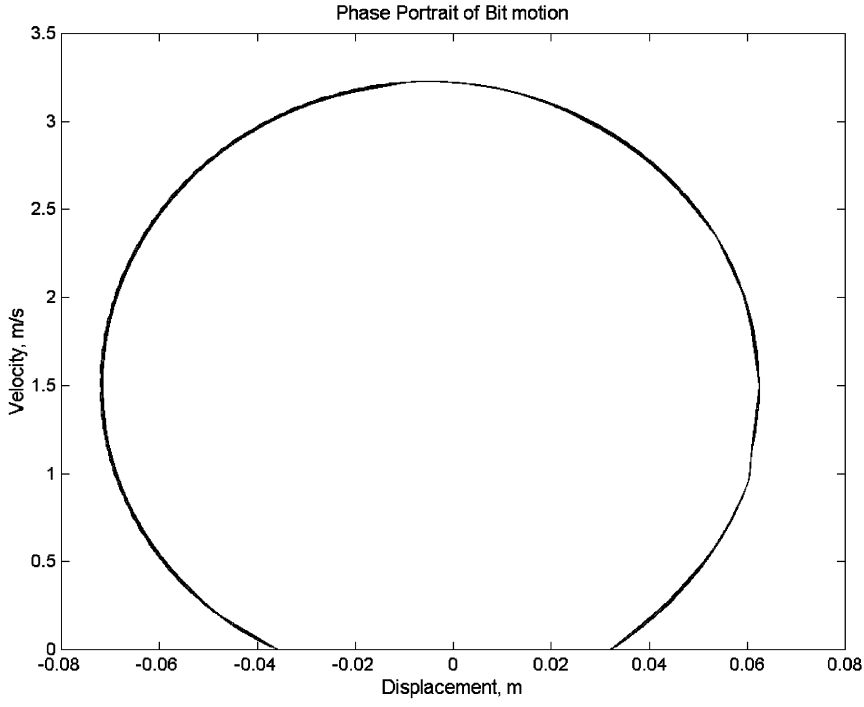

Figure 19. Phase portrait of bit motion for $\beta = 0{\cdot}1$.

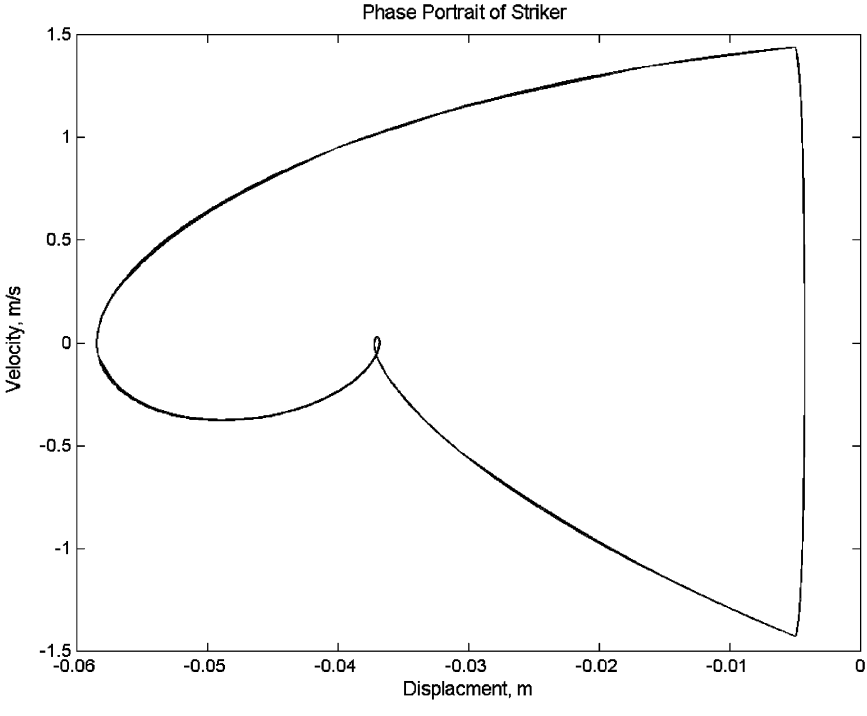

Figure 20. Phase portrait of striker motion for $\beta = 0{\cdot}1$.

Figure 21. Phase portrait of bit motion for $\beta = 0{\cdot}3$.

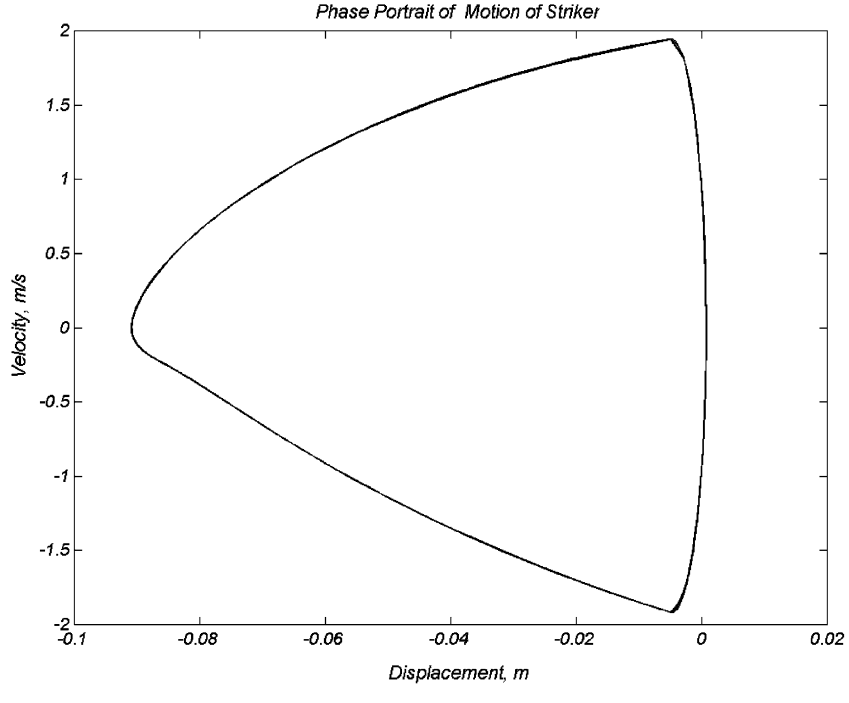

Figure 22. Phase portrait of striker motion for $\beta = 0{\cdot}3$.

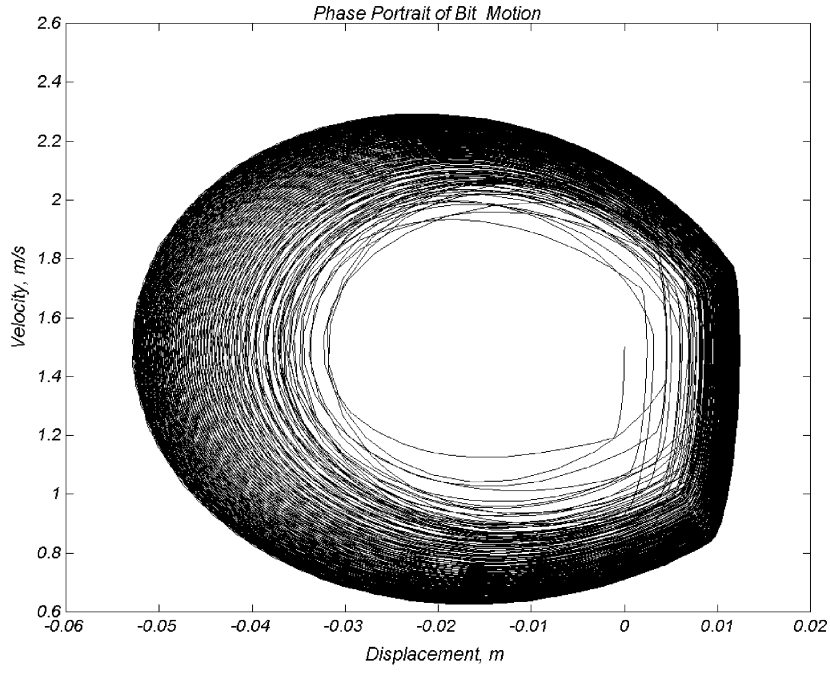

Figure 23. Phase portrait of bit motion for $\beta = 0{\cdot}6$.

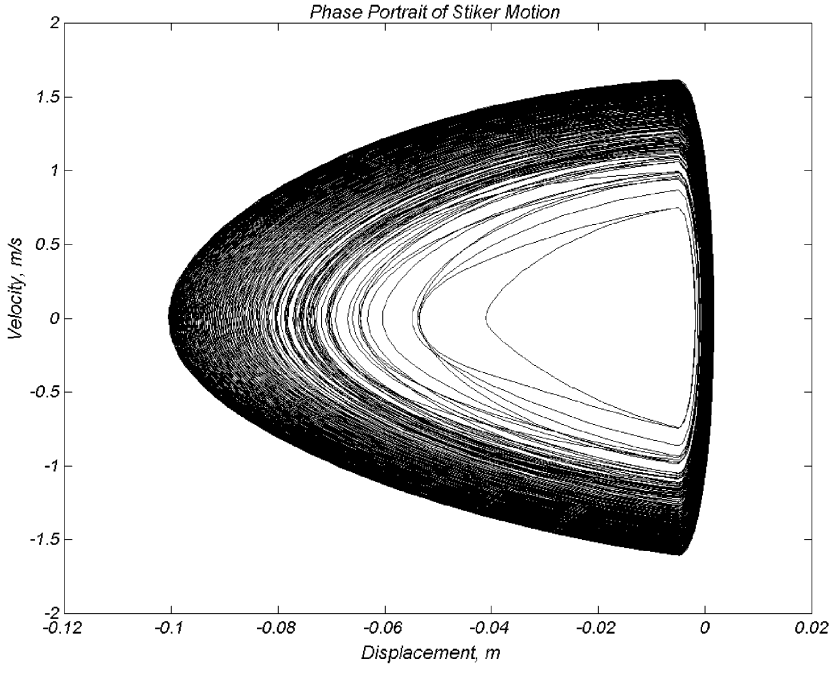

Figure 24. Phase portrait of striker motion for $\beta = 0{\cdot}6$.

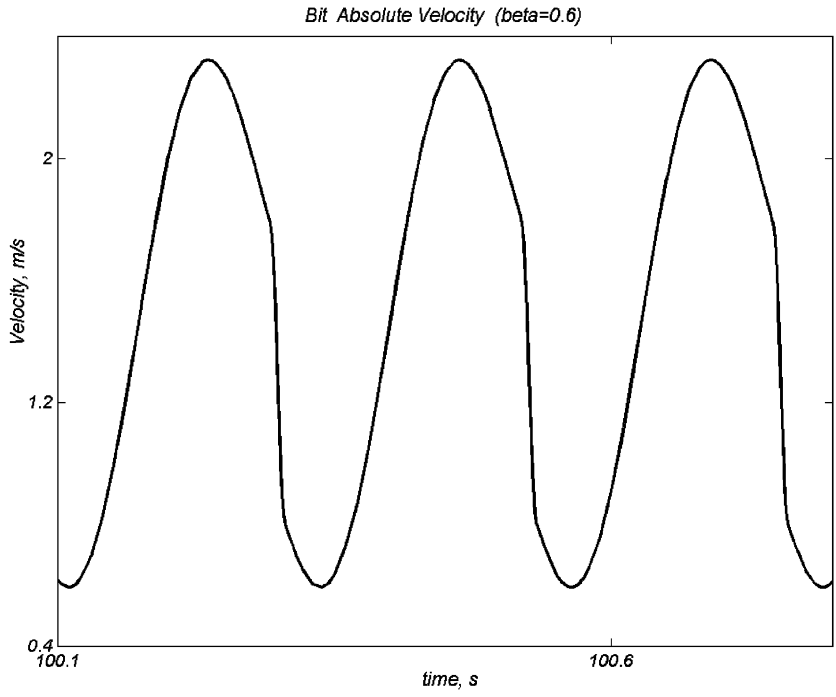

Figure 25. Bit absolute velocity for $\beta = 0{\cdot}6$.

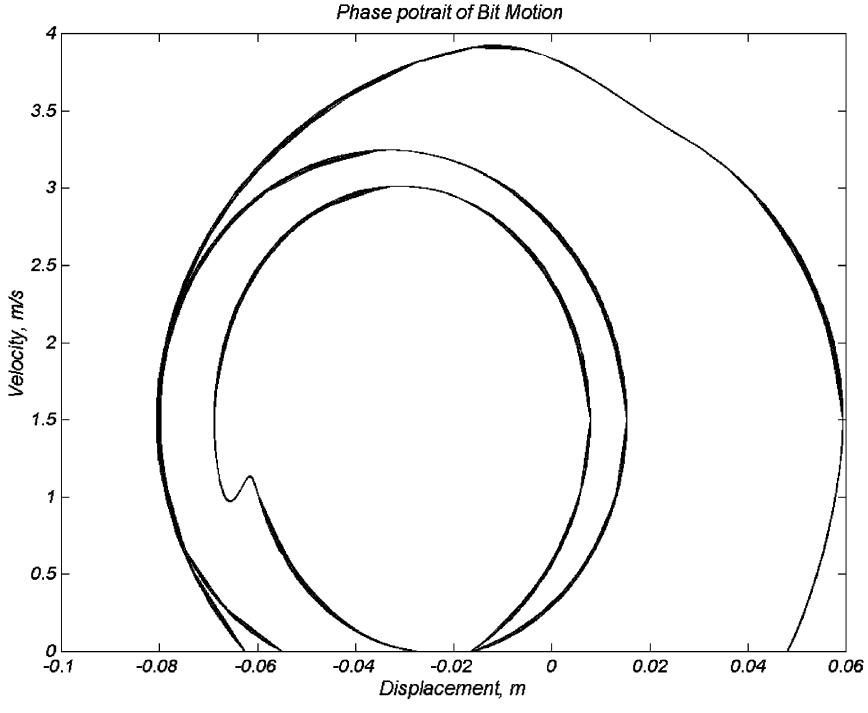

Figure 26. Limit cycle of bit motion for $\beta = 1{\cdot}3$.

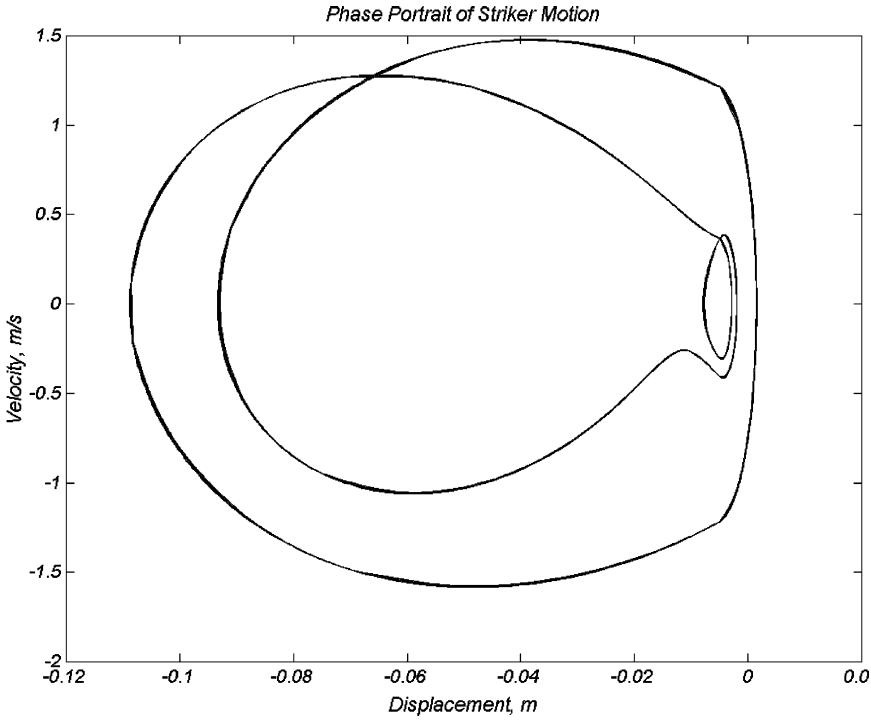

Figure 27. Limit cycle of striker motion for $\beta = 1{\cdot}3$.

For $\beta \geqslant 1{\cdot}3$: the system displays a bifurcation regime with three cycles. Figures 26 and 27 show this phenomenon where weak impact occurs only in the inner cycle.

5. CONCLUSIONS

The analysis presented in this paper defines a new concept of percussive-rotary drilling as a self-oscillatory process excited through the interaction between the multi-mass dynamical system and the medium being treated. The use of a natural mechanism for transformation of the energy of a standard rotation drive into the self-oscillatory percussive-rotary process of the drill bit brings adaptive features into the system without the need for measuring and control facilities. Correct tuning of the system permits the desirable correlation between the superimposed impacts and sticking, and sliding phases of the self-oscillatory process for achieving the best drilling performance.

It is clear that the decoupling mechanism must not induce any axial oscillation of the drill string. The initial design concept allows avoiding the use of torsional spring in the decoupling device, thus axial displacement of the string is not considered at this stage of investigation. The use of driving energy for excitation of the hammer during the sticking of drill bit relieves the main drive from dynamic loading and permits effective organization of vibration protection of the drill string. The system displays a self-adjustment property, which is to 'automatically' regulate resistance of the media being drilled. The vibro-impact activity of the decoupling device depends on the current value of the frictional force, whose threshold value is defined by the loading.

The numerical tools developed allow the system parameters to be calculated to provide an optimum design. It was revealed that the percussive-rotary self-oscillatory process of the system tends to a limit cycle with a frequency equal to the partial frequency of the bit estimated as $\sqrt{(k_1 + k_2)/m_1}$. To obtain a steady state vibro-impact process, the frequency ratio ω_2/ω_1 must be in a range of 0·75–0·8. The mass ratio β has a strong influence on the system response in terms of stability and performance. A value of β within an interval of 0·25–0·4 gives a stable operating mode, which allows the design of the new vibro-impact drilling mechanisms.

REFERENCES

1. I. Finnie and J. J. Bailey 1960 *American Society of Mechanical Engineers Journal of Engineering for Industry* 129–135. An experimental study of drillstring vibration.
2. P. R. Pasley and D. B. Bogy 1963 *American Society of Mechanical Engineers Journal of Engineering for Industry* 187–194. Drill string vibration due to intermittent contact of bit teeth.
3. D. W. Dareing and B. Livesay 1968 *American Society of Mechanical Engineers Journal of Engineering for Industry* 1–9. Longitudinal and angular drillstring vibration with damping.
4. R. F. Mitchell and M. B. Allen 1985 *World Oil* 101–104. Lateral vibration: the key to BHA failure analysis.
5. J. Kaski 1993 *Proceedings of the 4th Biennaial ASME Design Technical Conference on Vibration and Noise, Albuquerque, MN*, DE-60, 355–362. On the generation of bending vibration in drilling rod.
6. M. A. Elsayed, D. W. Dareing and M. A. Vonderheide 1997 *American Society of Mechanical Engineers Journal of Energy Resources Technology* **119**, 11–19. Effect of torsion on stability, dynamic forces, and vibration characteristics in drillstrings.
7. G. F. Brett 1992 *Society of Petroleum Engineers Drilling Engineering* **7**, 168–174. The genesis of torsional drillstring vibration.
8. J. D. Jansen and L. Van Den Steen 1995 *Journal of Sound and Vibration* **174**, 647–668. Active damping of self-excited torsional vibration in oil well drillstrings.
9. J. D. Jansen 1991 *Journal of Sound and Vibration* **147**, 115–135. Non-linear rotor dynamics as applied to oilwell drillstring vibration.
10. J. D. Jansen 1992 *Society of Petroleum Engineers Drilling Engineering* **7**, 107–114. Whirl and chaotic motion stabilized drill collars.
11. A. Kyllingstad and G. W. Halsey 1988 *Society of Petroleum Engineers Drilling Engineering* **3**, 369–373. A study of slip stick motion of the bit.
12. R. P. Dawson, Y. Q. Lin and P. D. Spanos 1987 *Spring Conference of the Society for Experimental Mechanics*. Drill string stick–slip oscillations. Houston.
13. F. J. Brett 1991 *SPE/IADC Drilling Conference, Amsterdam*. The genesis of bit-induced torsional drillstring vibrations.
14. M. P. Dufeyte Henneuse 1991 *SPE/IADC Drilling Conference, Amsterdam*. Detection and monitoring of the stick-slip motion: field experiment.
15. B. G. Fish 1956 *Mining Magazine*, March, 133–142. Percussive-rotary drilling.
16. W. D. Lacabanne and E. P. Pfleider 1955 *Mining Engineering* **7**(9), 850–855. Rotary percussion blasthole machine may revolutionize drilling.
17. R. Stribeck 1902 *Zeitschift des Vereins deutscher Ingenieure* **46**, 1342–1348, 1432–1337. Die wesentlichen Eigenschaften der Gleit- und Rollenlager. The key quantities of sliding and roller bearing.
18. V. I. Babitsky 1998 Theory of Vibro-impact Systems and Applications. Berlin: Springer-Verlag. (Revised translation from Russian. Moscow: Nauka, 1978.)
19. V. I. Babitsky and A. M. Veprik 1998 *Journal of Sound and Vibration* **218**, 269–292. Universal bumpered vibration isolator for severe environment.
20. S. A. Soundranayagam 2000 *Ph.D. Thesis*, *Loughborough University*, *UK*. Investigation of nonlinear transformation of impulses in impact units for improvement of hammer drill performance.